vienna2006

P027

Interaction of Low-Frequency Tube Waves with Poroelastic Reservoirs Containing Perforations

S.R. Ziatdinov* (St.-Petersburg University), A.V. Bakulin (Shell International Exploration and Production Inc), B. Gurevich (Curtin University of Technology) & R. Ciz (CSIRO Petroleum)

SUMMARY

Tube or Stoneley wave is known to strongly interact at low frequencies with poroelastic formations provided that flow is not restricted at the borehole-formation interface. Increased permeability leads to increased attenuation and decreased velocity of the tube wave. In this study we focus on reflection of low-frequency tube waves from various finite-size poroelastic structures. First, we examine a model of a thin reservoir and demonstrate good applicability of the approximate 1D effective wavenumber approach to describe interaction of tube waves with porous formations. We confirm that higher permeability leads to higher reflection coefficient. Then we analyze model of an idealized (disk-shaped) perforation inside a poroelastic layer and show that it has higher reflectivity compared to washout zone of the same geometry but with no-flow conditions at the face.

Introduction

Low-frequency tube waves are usually considered as a biggest source of noise in borehole seismic surveys. In acoustic logging high-frequency tube waves (or Stoneley waves) are useful to characterize the propreties of fractures and permeable zones since tube waves are sensitive to their permeability (Winkler et al., 1989; Tang and Cheng, 1993; Kostek et al., 1998). In cased boreholes tube waves can be used for qualitative estimation of quality and parameters of hydraulic fractures (Medlin and Schmitt, 1994; Paige et el., 1995). To obtain physical insight into the problem, White (1983) suggested a new approximate approach, based on 1D wave equation, that provides simple analytical description of the reflection and transmission of tube waves in the borehole. This 1D approach was verified using modeling of low-frequency tube waves in an open hole surrounded by elastic formations. In our study we verify this approach for poroelastic layers and extend it to describe the reflection response of an idealized disk-shaped perforation. Our study is a first step towards the quantitative interpretation of influence of formations and fracture properties in cased perforated holes on tube-wave propagation (Medlin and Schmitt, 1994; Paige et el., 1995).

1D effective wavenumber approach

This study focuses on the theoretical analysis of the interaction of tube (Stoneley) waves, propagating along a fluid-filled borehole, with elastic and poroelastic layers embedded between two elastic formations (Figure 1). We adopt the 1D approach originally proposed by White (1983) and generalized by Tang and Cheng (1993). This formulation is quite general and no restrictions are placed on the nature of the borehole structures, except for radial symmetry. The theory is able to treat the tube-wave interaction with different borehole structures such as elastic layers, permeable porous layers as well as diameter changes (washouts). In each homogeneous zone propagation is described by a 1D wave equation with constant effective wavenumber that depends on the properties of the surrounding formation as well as borehole parameters. To obtain the amplitudes of upgoing and downgoing waves, mass-balance boundary conditions are set at each interface, in particular, continuity of the fluid pressure and of the fluid displacement. In the low-frequency regime, reflection and transmission coefficients from a single layer of any type are given by:

$$R = \frac{2i\left(k_2^2 - k_1^2\right)\sin(k_2 L)}{\left(k_1 + k_2\right)^2 e^{-ik_2 L} - \left(k_1 - k_2\right)^2 e^{ik_2 L}}, \qquad (1)$$

$$T = \frac{4k_2 k_1 e^{-ik_1 L}}{\left(k_1 + k_2\right)^2 e^{-ik_2 L} - \left(k_1 - k_2\right)^2 e^{ik_2 L}}, \qquad (2)$$

where L is the layer thickness, k_1 is the axial Stoneley wavenumber in the two half-spaces and k_2 is the axial Stoneley wavenumber in the layer. These expressions are valid for a layer of any type as the rheology of the medium is absorbed by the effective wavenumber (Tang and Cheng, 1993). That is why we call this approach "effective wavenumber approach".
Stoneley wave propagation in the permeable zone is characterized by the effective wavenumber k_2:

$$k_2 = \sqrt{k_e^2 + \frac{2i\rho_f \omega \kappa(\omega)}{\Re \eta}} \sqrt{\frac{-i\omega}{D}} \frac{K_1(\Re\sqrt{-i\omega/D})}{K_0(\Re\sqrt{-i\omega/D})}, \qquad (3)$$

where K_1 and K_0 are modified Bessel functions of the second kind of the order one and zero, $\Re$ is the borehole radius, $\kappa(\omega)$ is the dynamic permeability, $D = \frac{\kappa(\omega)\rho_f c_f^2}{\phi\eta(1+\xi)}$ is the pore fluid diffusivity, ϕ is the porosity, ρ_f is the pore fluid density, c_f represents acoustic velocity of the pore fluid and ξ is a correction for the pore matrix compressibility (Chang et al., 1988). k_e is the wavenumber of the tube wave in an equivalent elastic formation given by

$$k_e = \frac{\omega}{c_T} = \omega\sqrt{\rho_f\left(\frac{1}{K_f}+\frac{1}{\mu}\right)}, \qquad (4)$$

with K_f being fluid bulk modulus and μ formation shear rigidity.

At seismic frequencies the tube wavenumber (3) becomes complex-valued, exhibits strong dependence on formation permeability and behaves very differently from its elastic analogue (4). The deviation from impermeable case is highest at lower frequencies and diminishes when frequency increases. Elevated attenuation and decreased tube-wave velocities are used as indicators for characterizing permeable zones in open-hole logging environment (Winkler et al., 1989).

Model of a thin reservoir

Let us examine the accuracy of the "effective wavenumber approach" for the case of poroelastic formations. Such comparisons have been previously reported for irregular borehole surrounded by elastic formations (Tezuka et al, 1997) and fluid-filled fractures (Kostek et al., 1998). In both cases effective wavenumber approach was shown to be in good agreement with direct computation of the wavefields by numerical methods. We are not aware of similar comparisons for poroelastic layers. Material parameters in formation are: bulk modulus (K) 25.139 GPa, shear modulus (μ) 16.875 GPa, density (ρ) 2700 kg m^3; in fluid: bulk modulus (K) 2.25 GPa, density (ρ) 1000 kg m^3; in porous layer: grain bulk modulus (K_g) 37 GPa, grain shear modulus (μ_g) 44 GPa, grain density (ρ_g) 3150 kg/m^3, bulk modulus of dry matrix (K_0) 11.452 GPa, shear modulus (μ) 9.3368 GPa, porosity 0.35, permeability 0-10 Darcy, viscosity 0.001 Pa s. Borehole radius is 0.142 m, layer thickness 2.4 m.

Figure 2 (dashed lines) depicts tube-wave reflection coefficient as a function of frequency for the thin reservoir model with parameters mentioned above computed with the effective wavenumber approach. Open boundary conditions are assumed between the borehole and the layer. Increase in layer permeability causes greater freedom for wellbore fluid to flow in and out of the poroelastic layer, leading to a larger reflection coefficient. Figure 2 also shows that a similar curves obtained with a finite-difference code jointly developed by Keldysh Institute of Applied Mathematics and Shell. Reflection coefficients were estimated by taking spectral ratios of incident and reflected tube waveforms. Good agreement between the two sets of curves is obtained above 80-100 Hz indicating that the effective wavenumber approach does capture the most important features of tube-wave interactions with poroelastic formations. Below 100 Hz the spectral-ratio calculations become less stable due to diminishing amplitudes in the input signal with 1000 Hz central frequency.

Idealized perforated model

Given success in describing tube-wave interaction for a single poroelastic layer, we decided to explore more complicated models with multiple layers. In particular, we focus on "idealized perforation model" depicted on Figure 3. While the geometry and material parameters in this model are identical to those for the single-layer model of Figure 1, the key distinction is that two thirds of the interface between wellbore and porous layer is now closed to flow. Therefore fluid communication only occurs in the middle porous layer. Real perforation can be roghly thought of as a small cylinder placed perpendicular to the main borehole in a particular azimuth and thus it will have much more limited area of flow. For this reason we call our model "idealized (disk-shaped) perforation". Also we do not account here for the extra rigidity caused by the presence of steel casing in real boreholes, although in principle this should be possible. With all these limitations "idealized perforation model" is a useful first step since it can be easily treated by cylindrically symmetric approaches at hand: effective wavenumber scheme and radially symmetric poroelastic finite-difference code.

First let us examine interaction of the tube wave with a zero-length perforation ($w = 0$). From now on we fix the permeability of porous zone to 1 Darcy. Due to smaller area of fluid communication the magnitude of the reflection coefficent decreases compared to fully open case and lies in between curves for single poroleastic and single elastic layers (Figure 4). Recall that elastic layer is equivalent to sealed (unperforated) poroelastic one. Multi-layered structure eliminates sharp troughs that were present in cases of single elastic or poroelastic layer. Overall we see good sensitivity of the reflection coefficient to the relative portion of wellbore-layer interface open to flow.
Idealized perforation of a finite length causes stronger reflection, since in addition to open flow we now have change in the borehole diameter (Figure 5). If we close the flow at the boundaries of the perforation, then we end up with what is conventionally called washout zone or enlargement in the borehole diameter examined in details by Tezuka et al (1997). For this particular model the reflection coefficient from the washout zone is higher than that of zero-length perforation. Nevertheless, the reflection amplitude from the finite-length perforation is substantially larger than from the simple washout. Since geometry of the models with washout and finite-length perforation are identical, the difference between reflection curves (cyan and blue on Figure 5) represents pure effect of fluid flow into the porous layer via open perforation.

Conclusions

We have applied 1-D effective wavenumber approach to analyze interaction of low-frequency waves with stack of poroelastic and elastic layers. For the first time we have shown good agreement between responses obtained with 1-D approach and finite difference computations.
We also extended our anlysis to cylindrically symmetric borehole irregularities inside poroelastic layers. In particular, we have examined the reflection response of a single idealized (disk-shaped) peforation inside the poroelastic layer. We have shown that cases of fully open to flow porous layer, fully sealed (unperforated) and partially sealed layer with finite-width and zero-length perforation can be distinguished for sufficuiently large permeabilities of the formation. For finite-length perforations changes in borehole diameter further increase the reflection coefficent. Yet for the same geometry the washout (no-flow) and perforation (open flow) can still be distinguished by their low-frequency response. For models at hand we observe larger reflection response for the perforation than for the washout. Realistic perforation geometries are 3D and therefore cannot be directly handled by 2D approaches. More theoretical and experimental work is needed to establish proper 3D description of wave interaction with realistic cylinder-shaped perforations.

References

Chang, S. K., Liu, H. L. and Johnson, D. L., 1988, Low-frequency tube waves in permeable rocks, Geophysics, 53, 519-527.
Kostek, S., Johnson, D. L., Winkler, K. W., and Hornby, B. E, 1998, The interaction of tube-waves with borehole fractures, Part II: Analytical models: Geophysics, 63, 809-815.
Tang, X. M., and Cheng, C. H., 1993, Borehole Stoneley waves propagation across permeable structures, Geophysical Prospecting, 41, 165-187.
Tezuka, K., Cheng, C. H., and Tang, X. M., 1997, Modeling of low-frequency Stoneley-wave propagation in an irregular borehole, Geophysics, 62, 1047-1058.
White, J. E., 1983, Underground sound, Elsevier.
Winkler, K. W., Liu, H., and Johnson, D. L., 1989, Permeability and borehole Stoneley waves: Comparison between experiment and theory, Geophysics 54, 66–75.

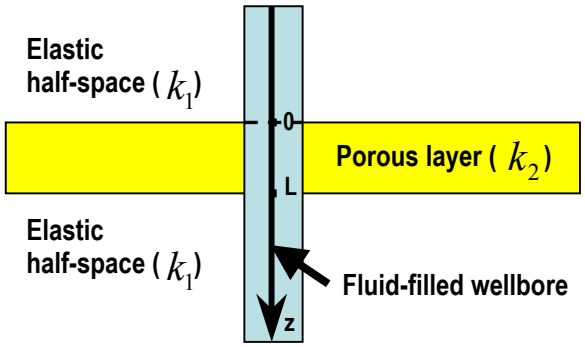

Figure 1: Model of fluid filled borehole intersecting a porous zone in an elastic formation.

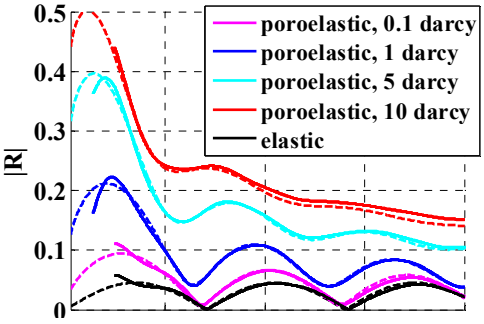

Figure 2. Amplitude of the tube-wave reflection coefficient as a function of frequency for a model with a single poroelastic layer (Figure 1). Dashed lines are derived with 1-D effective wavenumber approach, while solid lines are computed with finite-difference code. Bottom curve represents reflection from the elastic zone between two elastic half-spaces.

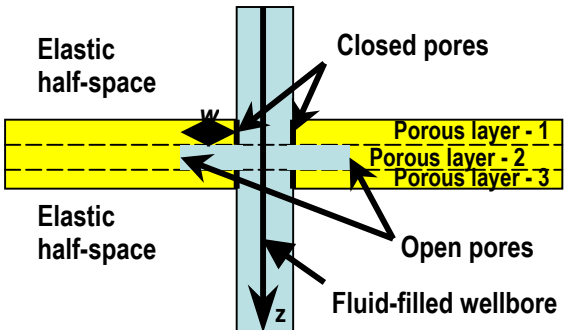

Figure 3: Idealized model of a disk-shaped perforation. All three porous layers have the same thickness (0.8 m) and identical material parameters. Layer 1 and 3 have closed boundary conditions preventing flow from and into the borehole

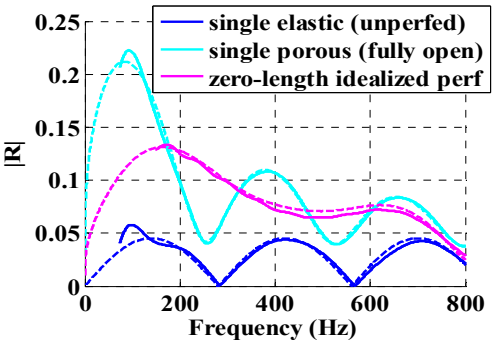

Figure 4: Reflection coefficient of the tube wave from the perforated and unperforated poroelastic layer. Dashed lines are derived with 1-D effective wavenumber approach, while solid lines are computed with finite-difference code.

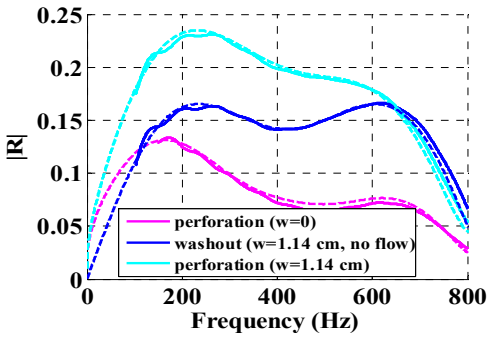

Figure 5: Reflection coefficient of the tube wave from a layer with a single idealized perforation of various lengths. Dashed lines are derived with 1-D effective wavenumber approach, while solid lines are computed with finite-difference code.